JOURNAL OF GEOPHYSICAL RESEARCH, VOL. 98, NO. B8, PAGES 13,863–13,877, AUGUST 10, 1993

Evolution of the Indian Ocean Triple Junction Between 65 and 49 Ma (Anomalies 28 to 21)

JÉRÔME DYMENT[1]

Institut de Physique du Globe, CNRS URA 0323, Université Louis Pasteur, Strasbourg, France

Reinterpretation of newly published geophysical data (Kamesh-Raju and Ramprasad, 1989) and older profiles of the Central Indian Basin, associated with similar studies of the Madagascar and Crozet basins, shows that the Indian Ocean Triple Junction trace on the Indian plate corresponds, at anomalies 23 and 22, to a N38°E offset of the magnetic lineations, oblique to both the Southeast Indian Ridge (SEIR) and Central Indian Ridge (CIR) spreading directions. The conjugate Triple Junction trace on the African plate identified in the Madagascar Basin is associated with a roughly north-south offset, parallel to the Southwest Indian Ridge (SWIR) fracture zones. In order to account for these observations and the velocity triangle of the Indian, African, and Antarctic plates close to the Triple Junction, a ridge-fault-fault mode is proposed, with a propagatorlike SEIR-CIR offset. The Triple Junction jumped between anomalies 24 and 23 and between anomalies 22 and 21, restoring a ridge-ridge-ridge configuration which immediately turned to a pseudo-ridge-ridge-fault and later to a true ridge-fault-fault configuration. After the Triple Junction jump at anomaly 21, the former SEIR-CIR offset was accommodated by a new CIR fracture zone. The lack of such a fracture zone prior to anomaly 21 suggests that either a pseudo-ridge-ridge-fault or an unstable ridge-ridge-ridge configuration prevailed before anomaly 24, in agreement with the velocity triangles which predict more unstable Triple Junction modes. Both modes support the creation of numerous SWIR fracture zones, presently observed between 52°30'E and 59°30'E, as a consequence of the Triple Junction evolution between anomalies 29 and 24. This result suggests that the physiography of the SWIR records the history of the Triple Junction.

INTRODUCTION

Three ridges and an associated triple junction define the plate geometry of the Central Indian Ocean since anomaly 34 [*Schlich,* 1982] (Figure 1). The Southeast Indian Ridge (SEIR), which separates the Indo-Australian and Antarctic plates, has the highest spreading rates. While it is now a typical intermediate rate spreading center, it was a fast spreading center between anomalies 31 and 22, with half spreading rates reaching 110 km/m.y. at anomaly 28 [*Patriat,* 1987; *Royer and Schlich,* 1988; *Munschy and Schlich,* 1989]. The Central Indian Ridge (CIR), which separates the African and Indo-Australian plates, is similar but displays slower spreading rates and a more complex geometry, particularly between anomaly 18 and present [*Fisher et al.,* 1971; *Patriat,* 1987]. The Southwest Indian Ridge (SWIR), which separates the African and Antarctic plates, is a slow spreading center and shows rough topography and large offset fracture zones [*Sclater et al.,* 1981; *Fisher and Sclater,* 1983].

On the basis of the few data available in the early 1970s, *McKenzie and Sclater* [1971] considered the Central Indian Ocean Triple Junction (TJ), also called the Rodriguez Triple Junction in its present configuration, to be a ridge-ridge-ridge (RRR) triple junction (R, ridge, and F, transform fault [after *McKenzie and Morgan,* 1969]). Until now, this assumption has remained valid at a regional scale. Subsequent investigations resulted in more accurate models describing the present-day TJ configuration and its evolution since anomaly 5. *Tapscott et al.* [1980] suggested a stable RRR configuration, with oblique spreading along the SWIR. *Patriat and Courtillot* [1984] proposed alternating RRR and RRF configurations, the RRR state corresponding to a magmatic mode and the RRF state to a tectonic mode.

SeaBeam data led *Munschy and Schlich* [1989] to reject the stable RRR configuration and to consider an unstable RRF configuration. In their model, the CIR and SEIR are being progressively offset at a rate of 1.4 km/m.y., mainly because of their different spreading rates. When the offset is large, the TJ jumps eastward and a new CIR segment is created. This behavior results in an overall constant length for the SEIR while the CIR lengthens. The SWIR also lengthens; nevertheless, the processes involved on the SWIR close to the TJ are more likely related to extension of the SEIR and CIR crusts than to normal seafloor spreading at the SWIR axis [*Patriat and Parson,* 1989; *Mitchell,* 1991]. Past readjustments of the TJ configuration are clearly evidenced from the SeaBeam bathymetry of the TJ trace on the Antarctic plate [*Munschy and Schlich,* 1989; *Patriat and Parson,* 1989] and also from magnetic and bathymetric data of the TJ trace on the Indian plate (TJT-In) [*Schlich et al.,* 1989].

The TJ evolution is therefore relatively well constrained for the past 10 m.y. From 10 to 43 Ma (anomaly 18), however, there is not enough geophysical data to carry out such detailed studies. Because the configuration of the three ridges appears not to have changed during this time span, it is reasonable to assume that the TJ configuration did not change. The TJ configuration before anomaly 18 is not as well understood; available data are sufficient to approximately define the trace of the TJ location [*Patriat and Segoufin,* 1988], but they are too sparse to accurately define the TJ geometry. *Patriat and Courtillot* [1984] derived the past relative positions of the spreading axes from paleogeographic reconstructions of the central Indian Ocean. As the reconstructions are consistent with a RRF configuration at

[1]Now at Earth and Planetary Sciences, McGill University, Montréal, Québec, Canada.

Paper number 93JB00438.
0148-0227/93/93JB-00438$05.00

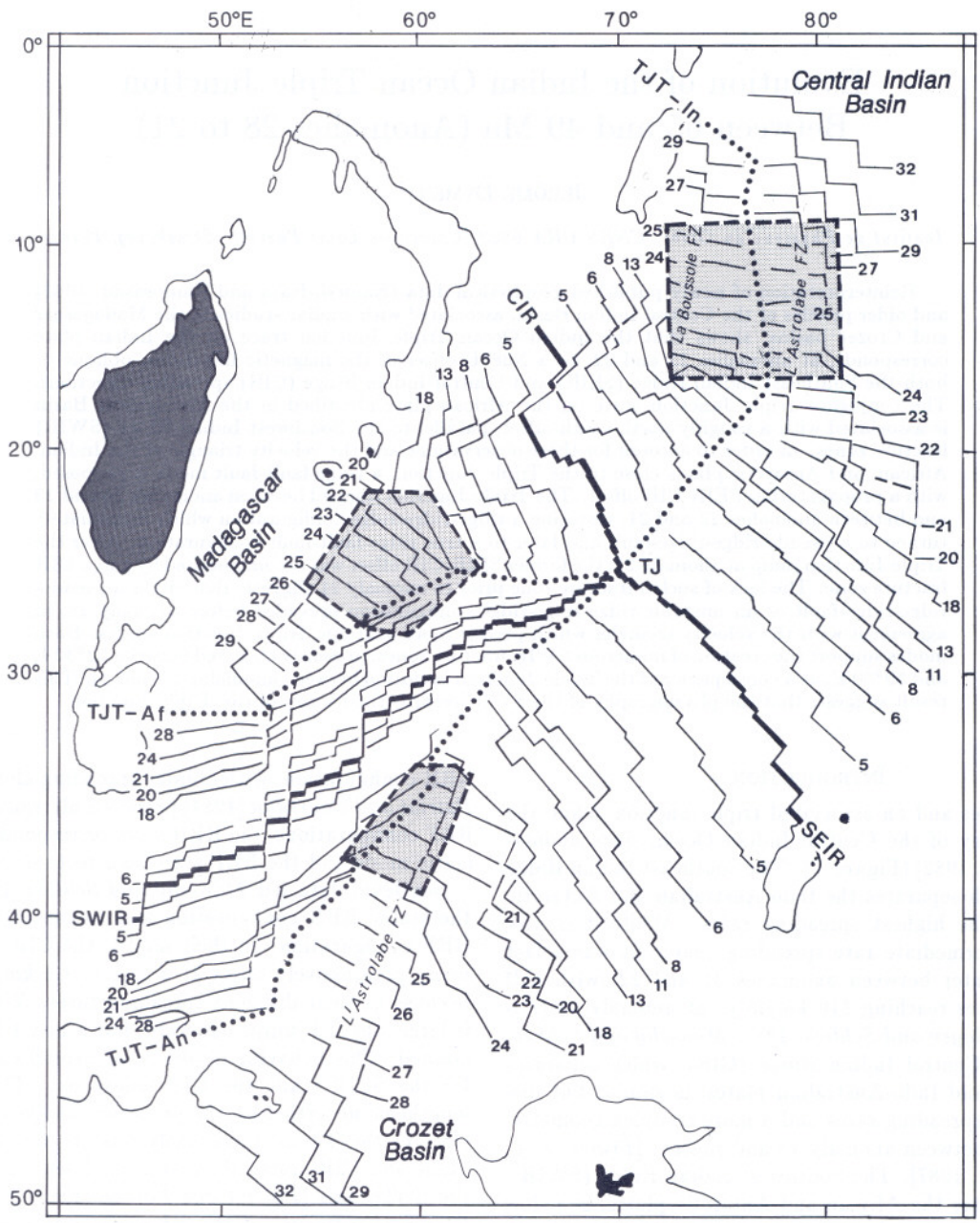

Fig. 1. Tectonic map of the Central Indian Ocean [after *Patriat and Segoufin,* 1988]. Thin lines are either isobath 2500 m or seafloor spreading isochrons with anomaly number; thick lines represent active spreading centers (CIR, Central Indian Ridge; SEIR, Southeast Indian Ridge; SWIR, Southwest Indian Ridge); dotted lines show Triple Junction traces (TJT) on the Indian (-In), African (-Af) and Antarctic (-An) plates; thick dashed lines contour the areas shown in Figures 2 and 5.

anomaly 28 and a RRR configuration at anomaly 24, they proposed alternating RRF and RRR configurations similar to their present-day TJ model.

New data in the Central Indian Basin were recently published by *Kamesh Raju and Ramprasad* [1989]. We use a combination of these and older data in this area to reexamine the past configuration and evolution of the TJ between anomalies 29 and 20, with special attention to the anomaly 24 to 21 interval. We will show that at some locations, the *Kamesh-Raju and Ramprasad* [1989] interpretation of the new data is not consistent with the older data.

Analysis of New Data in the Central Indian Basin

Between anomalies 29 and 20, the TJT-In lies in the Central Indian Basin, between two major fracture zones which *Patriat* [1987] named La Boussole Fracture Zone (FZ) and L'Astrolabe FZ (Figure 1). La Boussole FZ is located at about 74°E and lies on oceanic crust created at the CIR axis. L'Astrolabe FZ is located at about 79°E and separates two compartments of the SEIR; it is also called Indrani FZ by *McKenzie and Sclater* [1971]. Due to fast spreading of the SEIR and CIR and few magnetic reversals within this interval, magnetic anomalies are easy to identify.

New geophysical data in this area (Figure 2) were recently published by *Kamesh Raju and Ramprasad* [1989]. These data are located between La Boussole FZ and L'Astrolabe FZ, and between anomalies 24 and 21. Identifying the magnetic anomalies, *Kamesh Raju and Ramprasad* [1989] concluded that a fracture zone exists at 75°45'E. *Kamesh Raju and Ramprasad* [1989, p. 399] considered that "the postulated fracture zone [...] has strong implications on the evolution of the triple junction" but could not determine if this fracture zone is associated with the SEIR or the CIR.

Kamesh-Raju and Ramprasad [1989] assigned a N12°E direction to the fracture zones, which significantly differs from that proposed by previous workers. On the SEIR, *Sclater and Fisher* [1974] and *Sclater et al.* [1976] obtained a N6°E direction at anomaly 23 for L'Astrolabe FZ, while *Patriat*'s [1987] isochron map displays a N3°E direction at the same time. On the CIR, *Patriat* [1987] proposed a N12°E direction at anomaly 23 for La Boussole FZ. This discrepancy may be explained by the approximately N0°E orientation of the new tracks, which are subparallel to the fracture zones and cannot accurately resolve them. Some of the older data cut the fracture zones and allow a better determination of their location and orientation (Figure 2).

The magnetic anomaly identifications of *Kamesh Raju and Ramprasad* [1989] are consistent with those of *Sclater and Fisher* [1974] and *Patriat* [1987]. Nevertheless, the trends of their magnetic lineations are averaged over the different profiles, which lead to similar directions for the lineations created at the SEIR and CIR axes. Also, the abnormal shape of some magnetic anomalies (see, for example, anomaly 23 on profiles P 4 and P 5, Figure 2) are not considered in the interpretation. Consequently, the resulting scheme does not take into account oblique and asymmetric spreading, small-scale ridge jumps, and second-order ridge segmentation, which are likely to have existed on the fast or intermediate SEIR and CIR between anomalies 24 and 21. The Galapagos and Juan de Fuca ridges, which are intermediate spreading centers, show propagators [e.g., *Hey et al.*, 1980; *Wilson et al.*, 1984]; the East Pacific Rise, which is the only present-day fast spreading center, displays numerous overlapping spreading centers and other fine scale structures [e.g., *MacDonald et al.*, 1988]. While such struc-

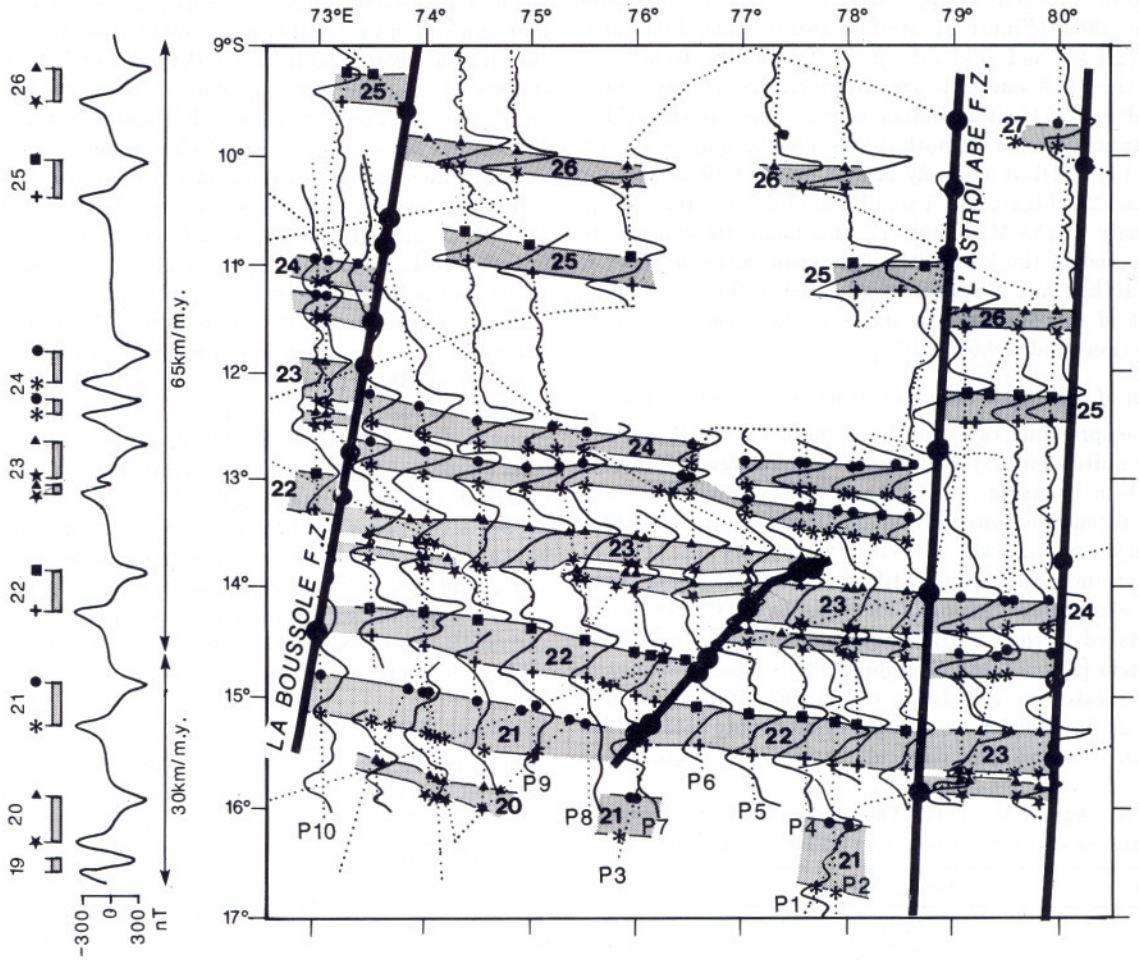

Fig. 2. (Right) Selected magnetic anomalies and tectonic interpretation in the Central Indian Basin. Anomalies are projected orthogonally to ship tracks, positive to the east. Data acquired by R/V *Jean Charcot*, *Marion Dufresne*, *Melville*, *Conrad*, and *Vema* are superimposed to recently published tracks (CIOB [*Kamesh-Raju and Ramprasad*, 1989]); all ship tracks are represented by dotted lines. Magnetic anomaly identifications are shown by symbols displayed on the synthetic profile; fracture zone or oblique offset identifications are represented by large dots. The positive magnetic polarity areas are shaded. (Left) Synthetic magnetic anomalies computed for oceanic crust created between 60 and 42 Ma (using geomagnetic reversal time scale of *Berggren et al.* [1985]) at 40°S along a ridge trending N120°E, observed at 10°S and 80°E along a N0°E profile, assuming magnetic prisms 6 km deep and 0.5 km thick and an equivalent 0.03 SI magnetic susceptibility.

tures are not recognizable in the other parts of the Central Indian Basin due to sparse data, second-order ridge segmentation, and small-scale ridge jumps can be resolved on the new data. We consider the data to be accurate enough to unambigously pick every magnetized block boundary. None of the ship tracks we use predates satellite navigation, and the accuracy of ship positioning is generally better than 2 km, as shown by errors measured at the crossing points located on a magnetic anomaly.

We have reinterpreted the new Indian data combined with the older French and American data. We picked every magnetized block boundary on every ship track and defined the trends of the magnetic lineations from every interpreted magnetic anomaly (Figure 2). Uncertainty in the trend of lineations was calculated as the standard deviation of azimuths between adjacent magnetic anomaly identifications, excluding recognized segmentations. Uncertainty in the trend of fracture zones represents the extreme possible directions allowed by magnetic anomaly identifications. We obtain a N3°E (±1°) direction for L'Astrolabe FZ and a N12°E (±1.5°) direction for La Boussole FZ, in agreement with *Patriat and Segoufin*'s [1988] results. Assuming that the TJT-In is located at approximatively 77°E [*Patriat and Segoufin,* 1988] (Figure 1), we find two distinct directions, N93°E (±1.5°) and N99.5°E (±2°), for the lineations created at the SEIR and CIR axes, respectively, and presently observed in the Central Indian Basin. Second-order ridge segmentation existed on both ridges; good examples can be seen on the SEIR at anomaly 22 and on the CIR at anomalies 23 and 24 (Figure 2). A small-scale ridge jump occurred at anomaly 23 (53 Ma, Table 1): this magnetic anomaly is not observed in the Central Indian Basin between 74°20'E and 75°10'E, while it appears duplicated in the corresponding part of the Madagascar Basin at 25°S and 58°E (see later sections and *Schlich* [1982]).

Location of the Triple Junction Trace on the Indian plate

As the spreading rate and direction of the SEIR and the CIR are quite similar, it is not easy to unambiguously locate the TJT-In by using only magnetic lineations. Paleogeographic reconstructions of former CIR and SEIR configurations may constrain the TJT-In, which likely lies between the easternmost anomaly identified in the Madagascar Basin and the westernmost anomaly identified in the Crozet Basin, both rotated to the Central Indian Basin using appropriate parameters [*Patriat and Segoufin,* 1988]. This constraint is used to locate the TJT-In on the magnetic lineation map (Figure 2), in addition to changes of spreading rate and/or direction. We also give particular attention to short-lived isochron discontinuities, which may represent the TJT-In in the case of unstable configurations [*Munschy and Schlich,* 1989; *Schlich et al.,* 1989].

TABLE 1. Age of Magnetic Anomalies 29 to 20, Following *Berggren et al.* [1985] Geomagnetic Reversal Time Scale

Anomaly	Young, Ma	Old, Ma
20	44.66	46.17
21	48.75	50.34
22	51.95	52.62
23	53.88	54.03
23a	54.09	54.70
24	55.14	55.37
24a	55.66	56.14
25	58.64	59.24
26	60.21	60.75
27	63.03	63.54
28	64.29	65.12
29	65.50	66.17

At anomaly 24, the TJT-In could lie either between profiles P 5 and P 6 or between profiles P 8 and P 9 (Figure 2): both places display a slight change in spreading rate and a bend of the magnetic lineations. However, only the first one adheres to the constraint given by paleogeographic reconstructions. At anomaly 23, the TJT-In lies between profiles P 4 and P 6, where a clear step of the spreading rate (which significantly increases eastward) is observed. The complex magnetic anomaly pattern observed on profiles P 4 and P 5 can be explained by an oblique NE-SW offset, the small "abnormal" magnetic anomalies observed on these profiles being aligned with CIR anomaly 23 identified on profiles P 6 and P 7. The same offset is observed at anomaly 22 on profiles P 7 and P 3, which display duplicated anomalies. A clear change of spreading direction, exceeding 5°, is located on this offset, interpreted as the TJT-In. Therefore profiles P 7 and P 3 successively cross, from south to north, the anomaly 22s created at the SEIR and at the CIR axes. Anomaly 21 is only identified on the western profiles P 8 to P 10. The younger limit of anomaly 21 is not seen on the southern end of profile P 8, probably because this profile lies on a fracture zone identified by *Patriat and Segoufin* [1988] (Figure 1). Farther east, anomaly 21 is recognized on profile P 3 at 76°E and on profiles P 1 and P 2 at 78°E. The TJT-In lies between these longitudes, as shown by the large eastward increase in spreading rate displayed by the data.

The previous analysis shows that the TJT-In is located at 77°40'E at anomaly 24, follows a linear N38°E (±2°) trend from 77°40'E at anomaly 23 old to 76°E at anomaly 22 young and is located between 76°20'E and 77°40'E at anomaly 21. Although this determination of the TJT-In is consistent with the constraint given by reconstructions [*Patriat,* 1987], the N38°E direction departs significantly from the N353°E trending TJT-In found by *Patriat* [1987] for this interval (Figure 1). This N38°E direction, controlled by at least 6 profiles (Figure 2), is likely related to a local structure observed only at anomalies 23 and 22. The interpretation supports two eastward TJ jumps, one between anomalies 24 young and 23 old, and the other between anomalies 22 young and 21 old. The TJT-In determined by *Patriat* [1987] averages such effects and schematizes the overall CIR lenghening and SEIR shortening, rather than describing the fine-scale TJT-In geometry.

Spreading Parameters

In order to accurately describe the trends of the SEIR and CIR magnetic lineations, we only considered the directions defined by data separated by 20 to 100 km. Small errors in navigation may cause important errors in trend determination by the use of intervals smaller than 20 km, as an uncertainty of ±1 km in the navigation of two 20 km spaced profiles may induce an uncertainty of 6° on the orthogonal trend. On the other hand, hidden second-order ridge segmentation is likely to affect intervals greater than 100 km. We also rejected intervals which include a recognized second-order ridge segmentation. Many directions are defined by more than three identifications (up to seven): as the second-order ridge discontinuities are commonly narrow, such redundant information helps to avoid misinterpretation of the trend of magnetic lineations. The average direction is N93.0°E for the SEIR and N99.5°E for the CIR, with stan-

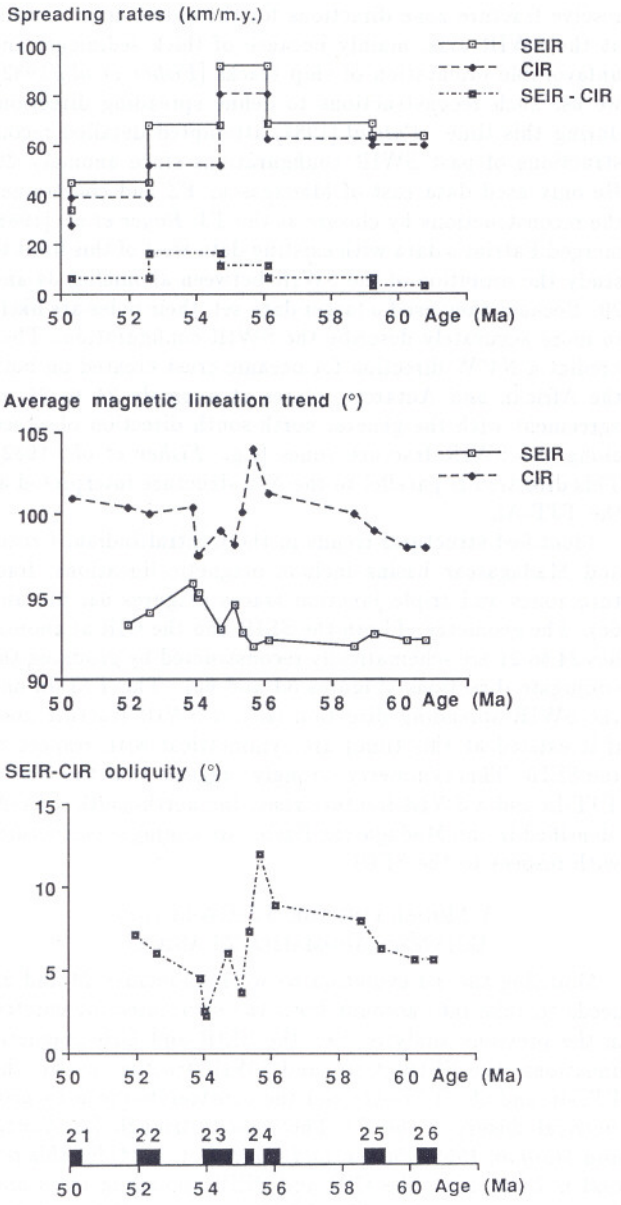

Fig. 3. Southeast Indian Ridge and Central Indian Ridge spreading rates (top) and magnetic lineation trends (center) versus time in the Central Indian Basin; Southeast Indian Ridge-Central Indian Ridge obliquity (i.e., difference of the magnetic lineation trends, bottom) versus time in the Central Indian Basin.

dard deviations of 1.5° and 2.0° respectively (Figure 3). The difference between the SEIR and CIR directions reaches 3.0° to 10.0°; the average value is 6.5°, with a standard deviation of 3.5°. These results are consistent with the 9° difference obtained between L'Astrolabe FZ and La Boussole FZ directions.

Figure 3 displays spreading rates and spreading center orientations of both the SEIR and CIR versus time. Spreading center orientations are determined for each magnetic reversal, while spreading rates are averaged over larger time spans in order to smooth errors due to uncertainties in both the location of the magnetic boundaries and the magnetic reversal time scale (such errors may be considerably amplified by using short magnetic polarity intervals). The time scale of *Berggren et al.* [1985] is used to compute the spreading rates.

Spreading rates show a similar evolution on both the SEIR and the CIR : they increased from about 64 km/m.y. on the SEIR (respectively 60 km/m.y. on the CIR) at anomaly 26 to 92 km/m.y. (80 km/m.y.) at anomaly 24, and then decreased to 34 km/m.y. (27 km/m.y.) at anomaly 21. Uncertainty on spreading rates averages 2 km/m.y. The difference between the SEIR and CIR spreading rates increased from 3 km/m.y. at anomaly 26 to 16 km/m.y. at anomaly 22 and then decreased to 6 km/m.y. at anomaly 21. Spreading center orientation displays a different evolution on the SEIR and the CIR. On the SEIR, it remained stationary at 92° between anomalies 26 and 24, increased to 96° at anomaly 23, and decreased to 93° at anomaly 22. On the CIR, it slightly increased from 98° at anomaly 26 to 104° at anomaly 24, sharply decreased to 97° between anomalies 24 and 23, and remained stationary at 100° until anomaly 21. Uncertainty on spreading center orientation does not exceed 2°. The SEIR-CIR obliquity increased from 6° to 12° between anomalies 26 and 24, decreased to 3° at anomaly 23, and again increased to 7° at anomaly 22.

Between anomalies 23 old and 22 young, the TJT-In coincided with a linear, N38°E offset. The nature and the role of this offset in the TJ evolution will be discussed later. We modeled the evolution of such an offset to check if this interpretation is consistent with spreading parameters. Isochrons were synthetized by using the previously determined spreading rates and directions; the SEIR and CIR isochrons were separated along N38°E boundary with an initial 40 km offset at anomaly 23 old, similar to the one measured on our interpreted ("real") isochrons (Figure 4).

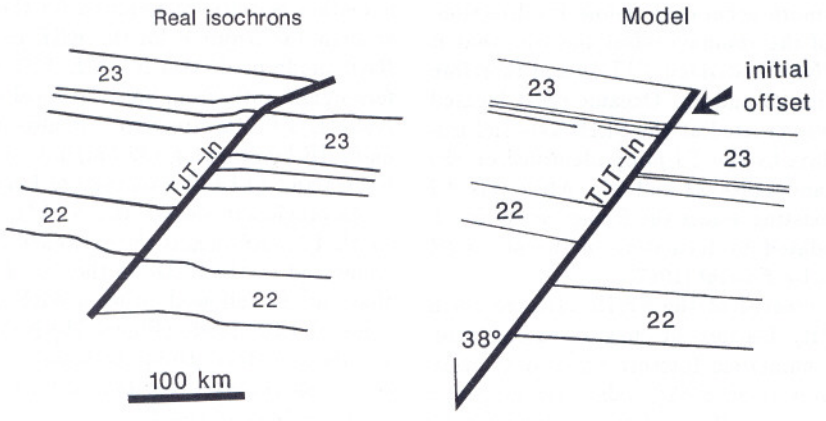

Fig. 4. Interpreted isochrons (left) and model (right) in the vicinity of the Triple Junction trace on the Indian plate.

Synthetic and real isochrons look quite similar (Figure 4), although differences exist in local variations of both spreading parameters and shape of the isochrons. Such effects are not randomly distributed but tend to maintain the SEIR-CIR offset constant at about 60 km. A good example is the creation of second-order ridge segmentation and the probable occurrence of spreading asymmetry between anomalies 23 and 22 (Figure 4).

CONSTRAINTS FROM THE MADAGASCAR AND CROZET BASINS

As in the Central Indian Basin, magnetic anomalies in the Madagascar and Crozet basins are easy to identify. *Schlich* [1975, 1982] interpreted magnetic anomalies 30 to 20 in the Madagascar Basin and 34 to 22 in the Crozet Basin. Our interpretation (Figure 5), based on an updated data set, does not significantly differ from *Schlich* [1982] and *Patriat* [1987]. We determined the direction and the length of the magnetic lineations for anomalies 24 to 21, both east of La Boussole FZ in the Madagascar Basin and west of L'Astrolabe FZ in the Crozet Basin. In the Madagascar Basin, magnetic lineations trend N129°E (±2°), and La Boussole FZ N39°E (±1°). The magnetic lineations are about 370 km long for anomalies 24 and 23 old. A more complex pattern is observed for anomalies 23 young to 20 and will be discussed later. In the Crozet Basin, the magnetic lineations trend N119°E (±3°), and L'Astrolabe FZ N29°E (±1°). The magnetic lineations are 220 km long for anomaly 24 old, 180 km long for anomalies 24 young and 23, and 100 km long for anomalies 22 and 21. The latter are, however, minimal estimates due to lack of data farther west (Figure 5). The lengths of magnetic lineations in the Madagascar and Crozet basins on one hand and in the Central Indian Basin on the other hand agree well. For example, anomaly 24 is about 600 km long in the Central Indian Basin, close to the sum of 370 and 220 km measured in the Madagascar and Crozet basins, respectively.

The part of the Madagascar Basin located between 24°S, 59°E and 26°S, 61°E should include the conjugate of the N38°E structure identified in the Central Indian Basin as the TJT-In, namely, the TJ trace on the African plate (TJT-Af). *Patriat* [1987] identified a CIR fracture zone which offsets anomalies 22 to 20. We also interpret a CIR fracture zone at anomaly 21 to 20 (Figure 5). South of 25°S, this N40°E fracture zone is continued by a roughly north-south structure which offsets anomaly 22. This linear feature is observed on five profiles. Our data are too sparse to follow it farther south or to more accurately define its direction. Nevertheless, the age of the anomaly offset suggests that it is the conjugate of the N38°E striking TJT-In and therefore the TJT-Af at anomalies 23 and 22. Oceanic crust located east of this structure was created at the SEIR axis and isolated on the African plate by the TJ jump identified on the Indian plate between anomalies 22 and 21. After this TJ jump, the large offset existing across the former north-south TJT-Af was accommodated by formation of the new CIR fracture zone identified by *Patriat* [1987].

Magnetic anomalies created at the SWIR axis are much more difficult to identify because of slow spreading rate, oblique spreading and numerous fracture zones [e.g., *Tapscott et al.*, 1980; *Sclater et al*, 1981]; individual magnetic anomaly interpretations generally need to be confirmed by paleogeographic reconstructions [*Patriat*, 1987; *De Ribet and Patriat*, 1988]. As bathymetric data do not accurately resolve fracture zone directions for the oldest crust created at the SWIR axis, mainly because of thick sediments and unfavorable orientation of ship tracks [*Fisher et al.*, 1982], we use such reconstructions to define spreading directions during this time. *Patriat* [1987] attempted detailed reconstructions of past SWIR configurations since anomaly 29. He only used data east of Madagascar FZ and constrained the reconstructions by closure at the TJ. *Royer et al.* [1988] merged Patriat's data with existing data west of this limit to study the evolution of the SWIR between anomalies 34 and 20. Because they used a larger data set, their poles are likely to more accurately describe the SWIR configuration. They predict a N4°W direction for oceanic crust created on both the African and Antarctic plates at anomaly 24 to 21, in agreement with the general north-south direction observed along the SWIR fracture zones [e.g., *Fisher et al.*, 1982]. This direction is parallel to the N-S structure interpreted as the TJT-Af.

Identified structural trends in the Central Indian, Crozet and Madagascar basins include magnetic lineations, fracture zones and triple junction traces (Figures 6a, 6b, and 6c). The geometry of both the SEIR and the CIR at anomalies 24 to 21 are schematically reconstructed by grouping the conjugate directions (Figures 6d and 6e). The TJT-In and the SWIR spreading direction (i.e., a SWIR fracture zone if it existed at this time) are symmetrical with respect to the SEIR. This symmetry strongly suggests that the N38°E TJT-In and a SWIR fracture zone, the north-south TJT-Af identified in the Madagascar Basin, are conjugate structures with respect to the SEIR.

A MODEL FOR THE TJ EVOLUTION BETWEEN ANOMALIES 24 AND 21

Modeling the TJ evolution between anomalies 24 and 21 needs to take into account both the structures interpreted in the previous analysis (i.e., the SEIR and CIR magnetic lineations; the SEIR, CIR, and SWIR fracture zones; the TJT-In and the TJT-Af) and the constraints given by geometrical closure at the TJ. The velocity triangle [*McKenzie and Morgan*, 1969; *Patriat and Courtillot*, 1984] for this period is built using the CIR and SEIR spreading rates and directions (Figure 7). The SWIR spreading direction predicted by closure at the TJ matches the one computed with *Royer et al.*'s [1988] pole, while the spreading rates only differ for 1 km/m.y.

In the framework of rigid plate tectonics, only the RRR mode (Figure 7a) can account for the velocity triangle, which is neither isoceles (as required for the RFF mode) or a right triangle (as required for the RRF mode). Nevertheless, the RRR mode predicts a N318°E TJT-In direction, which differs significantly from both the local N38°E and the regional N353°E TJT-In directions. It also implies very fast SWIR and CIR lengthening (39 km/m.y. and 33 km/m.y., respectively) and SEIR shortening (28 km/m.y.).

As previously shown, the N 38°E TJT-In and the north-south TJT-Af suggest the existence of a SWIR fracture zone connected to the SEIR at the TJ. This observation implies that the TJ followed either a RRF or a RFF mode at this time. A RRF mode (Figure 7b) is clearly inconsistent with the data, unless strong asymmetry and obliquity, not observed on the data, existed on both the SEIR and the CIR in the vicinity of the TJ.

A RFF mode (Figure 7c) agrees with SEIR, CIR and SWIR spreading directions and rates. It predicts reason-

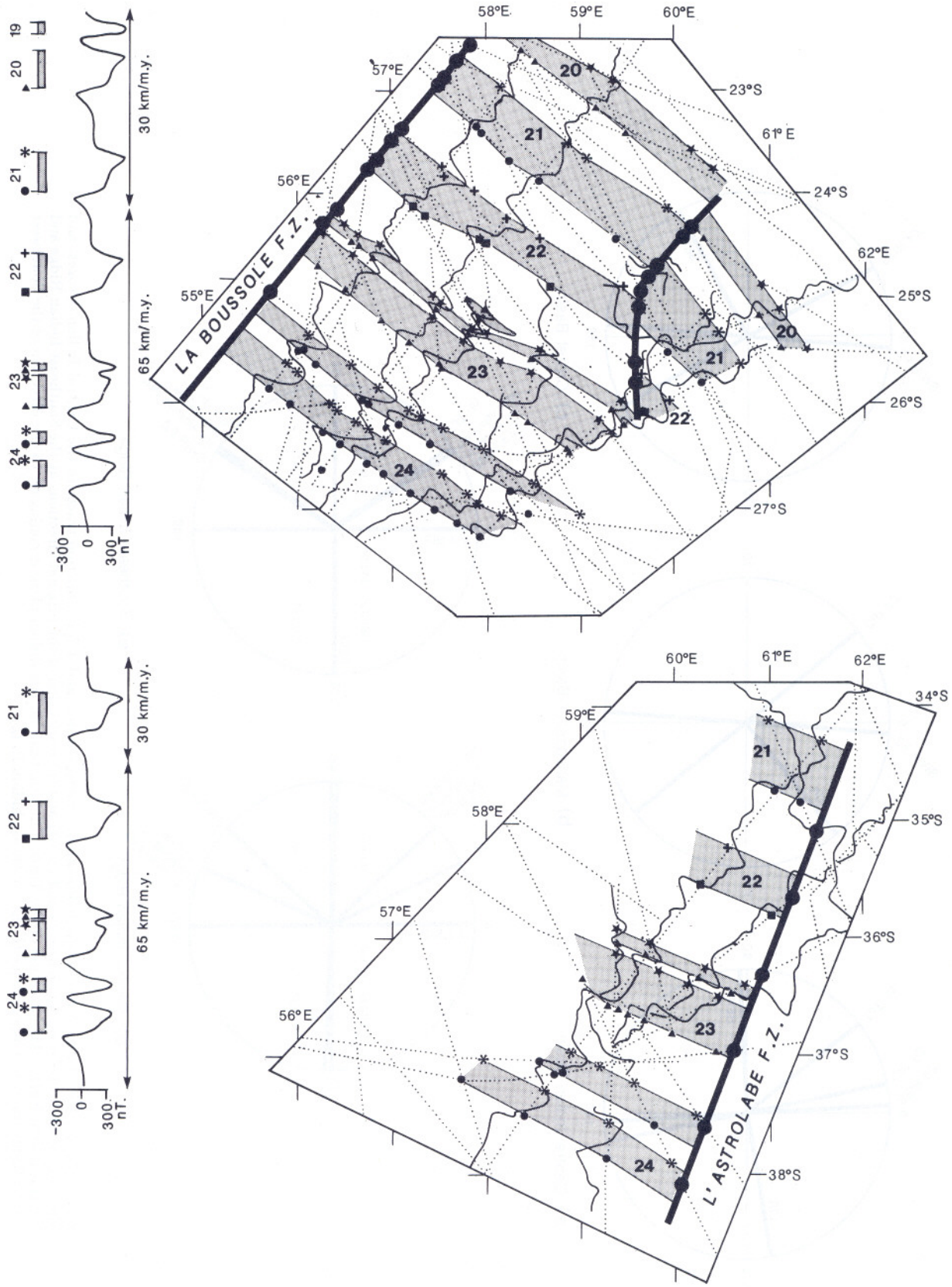

Fig. 5. (Right) Selected magnetic anomalies and tectonic interpretation in the Madagascar (top) and Crozet (bottom) basins. Anomalies are projected orthogonally to ship tracks, positive to the east. All ship tracks are represented by dotted lines. Magnetic anomaly identifications are shown by symbols displayed on the synthetic profile; fracture zone or oblique offset identifications are represented by large dots. The positive magnetic polarity areas are shaded. (Left) Synthetic magnetic anomalies computed for oceanic crust created between 61 and 44 Ma (using geomagnetic reversal time scale of *Berggren et al.* [1985]) at 40°S along a ridge trending N130°E fot the Madagascar Basin (N120°E for the Crozet Basin), observed at 25°S and 60°E (40°S and 60°E) along a N40°E (N30°E) profile, assuming magnetic prisms 6 km deep and 0.5 km thick and an equivalent 0.03 SI magnetic susceptibility.

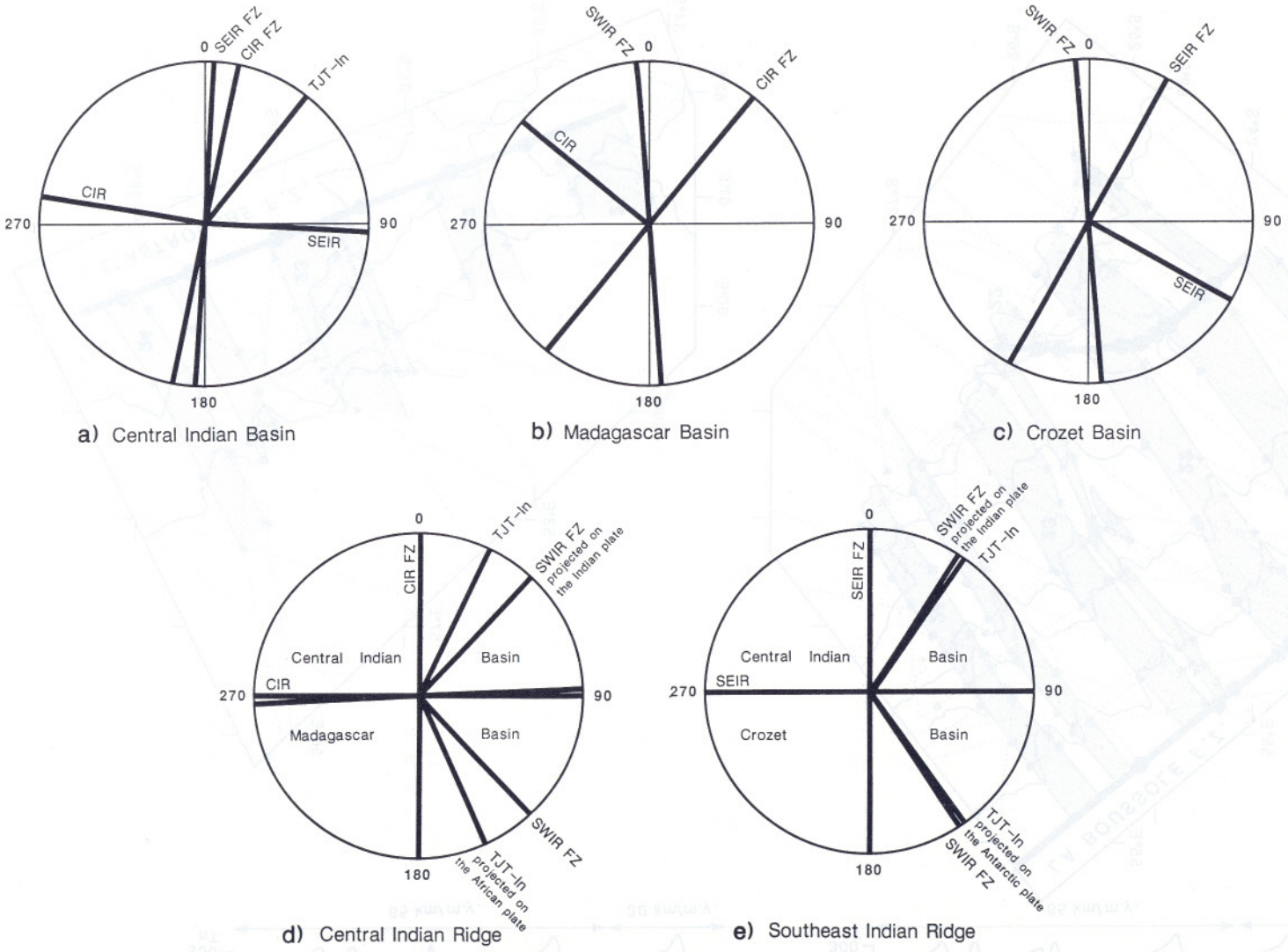

Fig. 6. (a)-(c) Directions of the magnetic lineations, fracture zones, and Triple Junction traces in the Central Indian, Crozet, and Madagascar basins between anomalies 24 and 21; (d) and (e) restitution of the original directions at the Southeast Indian Ridge and Central Indian Ridge. The direction of the Triple Junction trace on the Indian plate is conjugate to the direction of the Southwest Indian Ridge fracture zones relative to the Southeast Indian Ridge.

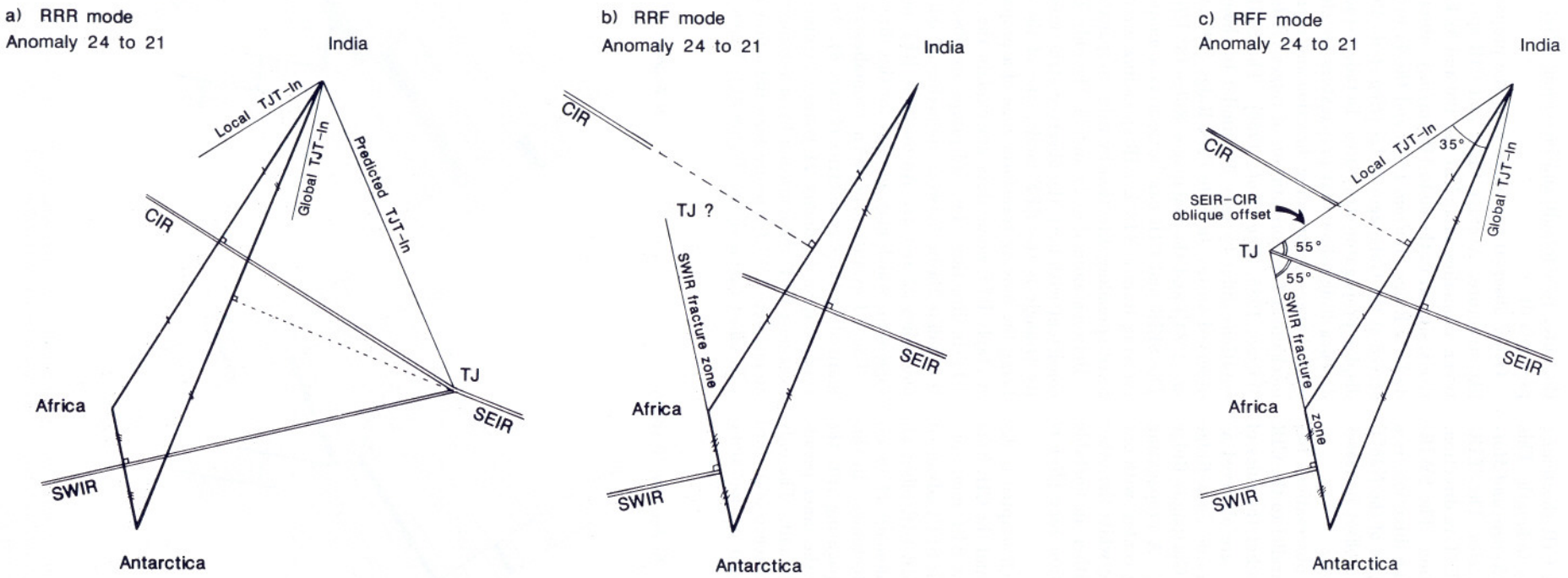

Fig. 7. (a) Ridge-ridge-ridge, (b) ridge-ridge-fault, and (c) ridge-fault-fault configurations applied to the velocity triangle between anomalies 24 young and 21 old.

able SEIR lengthening (14 km/m.y.) and CIR shortening (10 km/m.y.), while the SWIR is stationary in length. This mode is not a RFF mode sensu stricto [*McKenzie and Morgan,* 1969], as the velocity triangle is not isoceles. The SEIR-CIR offset, which accounts for the N38°E TJT-In direction, is not parallel to the CIR spreading direction. The SWIR-SEIR offset, parallel to the SWIR spreading direction, is a true SWIR fracture zone that is the conjugate of the N38°E SEIR-CIR offset. The SWIR fracture zone offset increases 3 or 4 times faster than the SEIR-CIR offset.

The RFF model is consistent with the observations but requires a SEIR-CIR offset which is not parallel to the CIR spreading direction, which seems to contradict the rules of plate tectonics. Oblique offsets, however , are observed as products of ridge propagation, on the Juan de Fuca Ridge [*Hey,* 1977; *Hey et al.,* 1980] and on the Galapagos Ridge [*Searle and Hey,* 1983; *Hey et al.,* 1986]. A propagating rift is a nonstationary offset of a spreading center, with one branch of the spreading center lengthening while the other recedes [*Hey,* 1977]. The offset itself is either an unstable transform fault or a distributed deformation zone [*Hey et al.,* 1980; *McKenzie,* 1986].

Such a propagating rift is particularly well adapted to describe the relationships between the SEIR and the CIR from anomaly 24 to 21. As previously shown, a RFF mode implies that the CIR receded westward and the SEIR advanced westward at the TJ. A propagatorlike SEIR-CIR offset allows for a RFF TJ configuration from anomaly 24 to 21, without contradicting the rules of plate tectonics. In this framework, the SEIR represents the propagating rift, the CIR the doomed rift, the N38°E TJT-In the inner pseudofault and the SWIR FZ the outer pseudofault. The only difference with true propagators is the existence of a third ridge, the SWIR, which results in transform motion along the outer pseudofault and increasing offset along the inner pseudofault.

Other observations agree with the proposed propagatorlike structure. Average SEIR and CIR spreading rates between anomalies 24 and 21 are 100 and 81 km/m.y., respectively, similar to the 60 to 110 km/m.y. observed at the Juan de Fuca Ridge [*Wilson,* 1988] and the 42 to 72 km/m.y. observed at the Galapagos Ridge [*Hey et al.,* 1977], which both display propagator structures. Detailed studies of the Juan de Fuca Ridge show that propagators are closely associated with changes in spreading direction and represent a possible mechanism for reorientation of ridges [*Wilson et al.,* 1984; *Wilson,* 1988; *Hey et al.,* 1988]. The SEIR and CIR orientations differ by only 9°, similar to changes of direction observed on the Juan de Fuca Ridge (10° to 15° [*Wilson et al.,* 1984]) and the Galapagos Ridge (8° [*Hey et al.,* 1986]). The SEIR and CIR can be seen as a unique ridge system, evolving from a N12°E CIR spreading direction to a N3°E SEIR spreading direction by ridge propagation.

Between anomalies 24 and 21, the only TJ configuration consistent with both the observed structures and the velocity triangle is the RFF mode, one of the transform fault being the moving transform zone of a propagatorlike offset. A stable RFF mode does not explain the regional N353°E TJT-In direction. Two TJ jumps are observed in the Central Indian Basin, between anomalies 24 and 23 and between anomalies 22 and 21. An unstable RFF mode is therefore suggested, which may account for this direction.

The TJ evolution between anomalies 24 and 21 is summarized by three geometries (Figure 8). An initial RRR TJ configuration (anomaly 24 young, Figure 8a) immediately became a RFF configuration by increasing offset along both an incipient SWIR fracture zone and a propagatorlike SEIR-CIR offset (anomaly 22, Figure 8b). When one of these off-

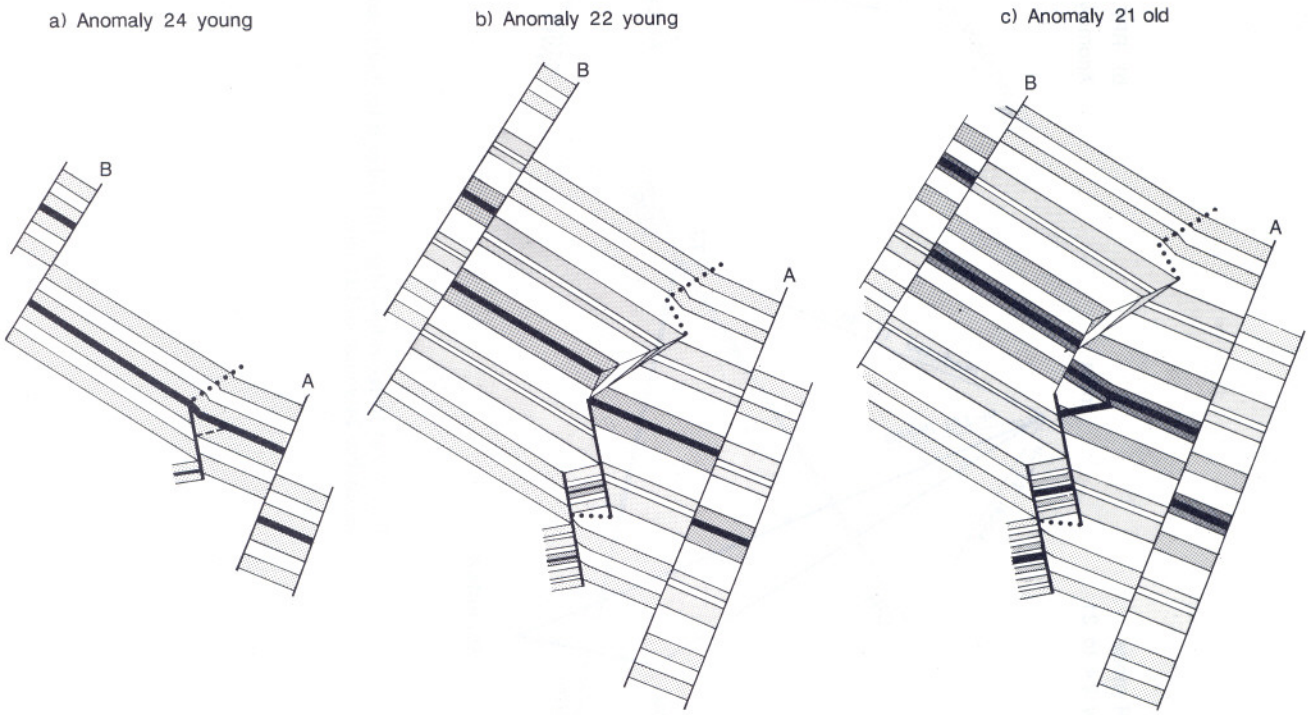

Fig. 8. Model for the Triple Junction evolution between anomalies (a) 24 young, (b) 22 young, and (c) 21 old following a ridge-fault-fault configuration with a propagatorlike Southeast Indian Ridge-Central Indian Ridge offset. A, L'Astrolabe FZ; B, La Boussole FZ.

sets reached a critical value, an eastward TJ jump created a new SWIR segment and restored the initial configuration (anomaly 21 old, Figure 8c). Such a predominant RFF configuration turning episodically to a transient RRR configuration has already been proposed for the Bouvet triple junction, which displays an isoceles velocity triangle compatible with both modes [*Kleinrock and Phipps Morgan,* 1988].

Both the SEIR-CIR offset and the SWIR fracture zone controlled TJ evolution. The offset along the SWIR fracture zone increased rapidly and disconnected the SWIR from the SEIR-CIR system. Therefore, the fine scale TJ configuration likely depended on the SEIR-CIR offset, which increased 3-4 times slower. Two different stages, related to the amount of this SEIR-CIR offset, can be distinguished (Figure 9). In the first stage, the offset was quite small and was compensated by small-scale ridge jumps, local obliquity and/or asymmetry or second order ridge segmentation. The TJ configuration was quite similar to the RRF mode and is therefore called "pseudo-RRF" mode. When the offset increased, it could not be further compensated in such a way. The transient pseudo-RRF mode evolved either to a true RFF mode, by the development of a propagatorlike SEIR-CIR offset, or to the initial RRR mode, by a TJ jump.

A true RFF mode prevailed between anomaly 23 and 22, followed by an eastward TJ jump which occurred before anomaly 21. As a consequence of this jump, a new CIR fracture zone was created to accommodate the offset accumulated since anomaly 23. This fracture zone is connected to the TJT-In and TJT-Af (Figure 8). Such a new CIR fracture zone creation is not observed on data between La Boussole FZ and the triple junction for oceanic crust older than anomaly 21. Moreover, the offset between SEIR and CIR magnetic lineations older than anomaly 24 seems much smaller than the one observed at anomalies 23 and 22. As no large SEIR-CIR offset existed, a pseudo-RRF mode likely prevailed before anomaly 23. The occurrence of a true RFF propagatorlike configuration between anomalies 23 and 22 may be related to the significant decrease in spreading rate observed on both the SEIR and CIR at anomalies 23 and 22 [*Patriat,* 1987]. These new spreading rates are indeed close to those presently observed at the Juan de Fuca and Galapagos ridges, which both display propagators. Before anomaly 23, the SEIR and CIR were quite similar to the present East Pacific Rise, which does not show such propagators.

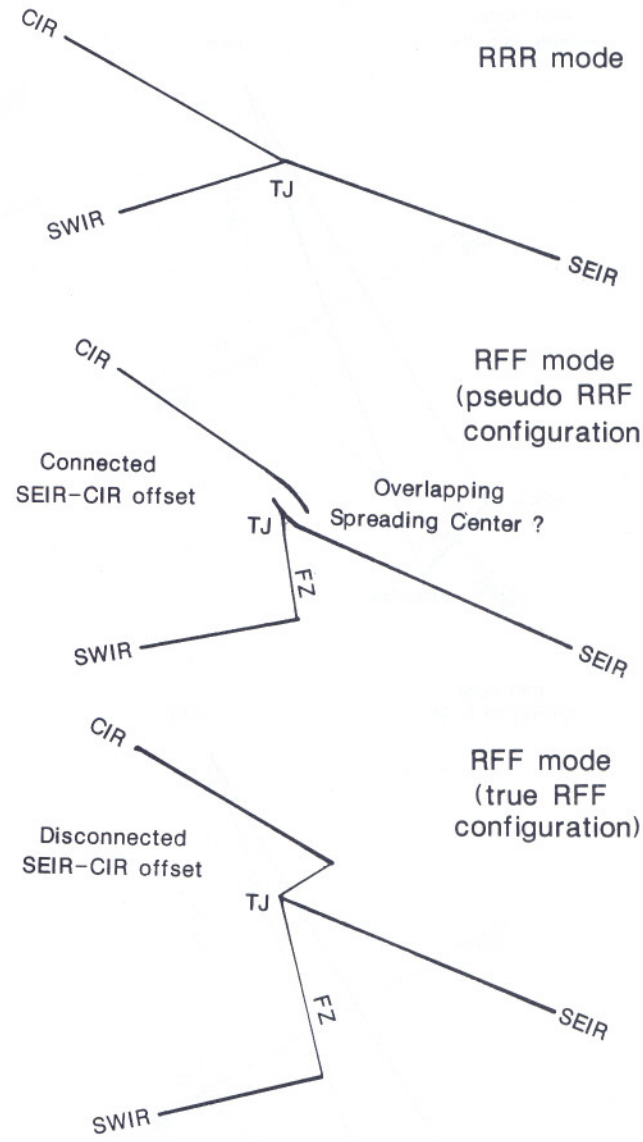

Fig. 9. Different stages of the evolution of a ridge-fault-fault configuration with a propagatorlike offset: instantaneous ridge-ridge-ridge configuration, transient pseudo-ridge-ridge-fault configuration, true ridge-fault-fault configuration.

GENERALIZATION TO ANOMALY 28 TO 24 AND IMPLICATIONS OF THE MODEL

Dense data in the Central Indian Basin allow us to propose a new model for TJ evolution between anomalies 24 and 21. No major change in the SEIR, CIR, and SWIR configurations seems to have occurred in the vicinity of the TJ between anomalies 29 and 24, and the TJ may have followed a similar evolution during this time. We have already noted that a SEIR-CIR offset at the TJ resulted in the creation of a new CIR fracture zone when the TJ jumped eastward. As such fracture zones are not observed in the Central Indian Basin before anomaly 21, no large SEIR-CIR offset existed before anomaly 24; a pseudo-RRF mode is therefore considered.

In order to test this hypothesis, velocity triangles were computed for two periods, one between anomalies 28 young and 26 old, the other between anomalies 26 old to 24 old (Figure 10). Average spreading rates and directions were directly measured from data in the Central Indian Basin for the SEIR and the CIR. The SWIR spreading rate and direction predicted by closure at the TJ and computed from *Royer et al.* [1988] parameters of rotation agree between anomalies 28 and 26 but differ by 12° and 3 km/m.y. between anomalies 26 and 24. This discrepancy may be related to difficulties in identification of anomaly 26 on the SWIR (P. Patriat, personal communication, 1991).

Velocity triangles are consistent with a RRR mode (Figure 10). This mode implies rapid SWIR lengthening (35 to 42 km/m.y.) and slower CIR lengthening (17 to 23 km/m.y.) and SEIR shortening (11 to 16 km/m.y.). The RFF mode is also possible, assuming the SEIR-CIR offset to be oblique with respect to the CIR spreading direction (Figure 10). This mode predicts a fast SEIR lengthening (about 60 km/m.y.) and CIR shortening (about 40 km/m.y.), and it leads to a fast increase of the offset (about 60 km/m.y.) at the SWIR fracture zone. It also implies that the TJT-

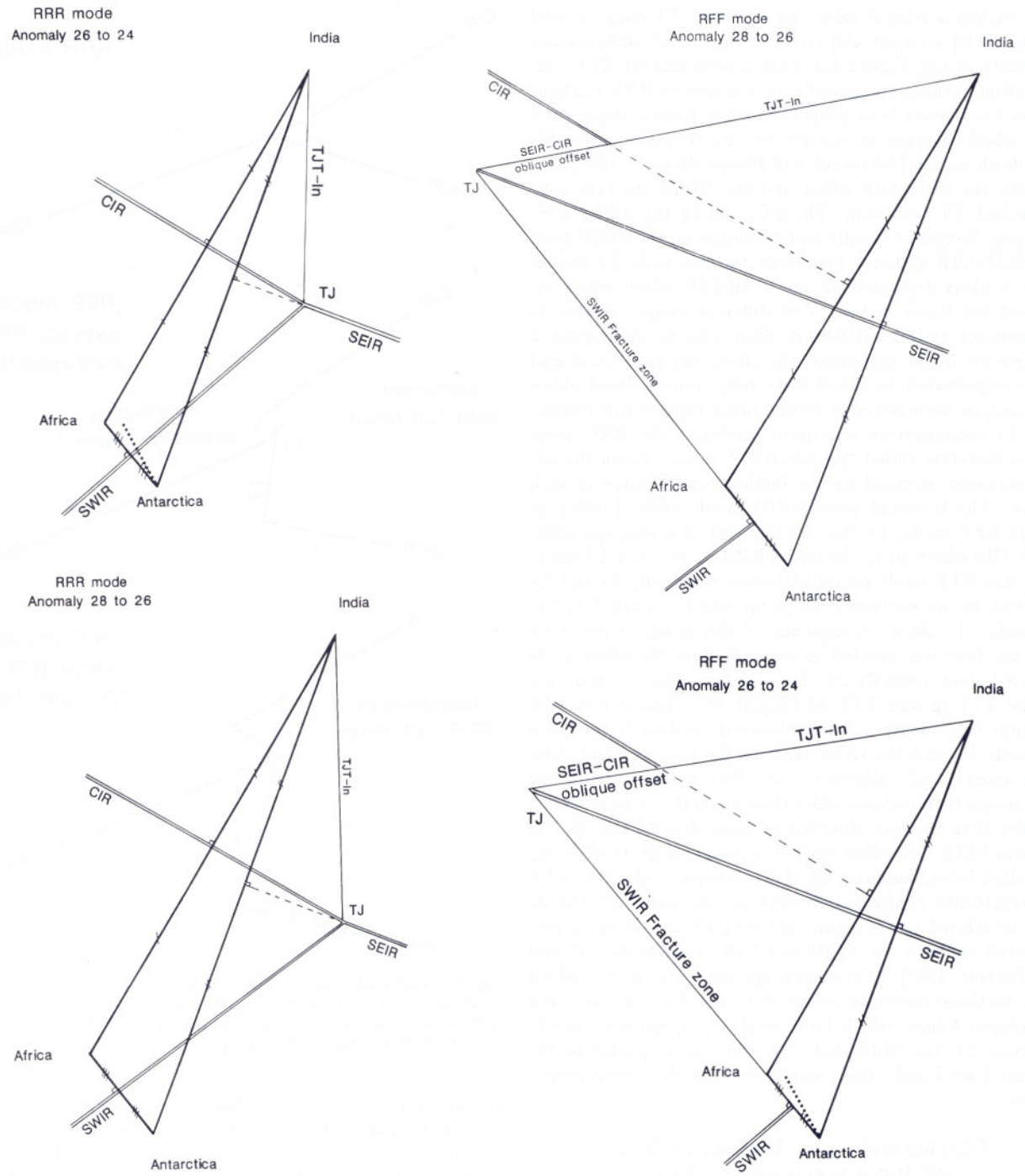

Fig. 10. (left) Ridge-ridge-ridge and (right) ridge-fault-fault configurations applied to the velocity triangle between (top) anomalies 26 old and 24 young and (bottom) anomalies 28 old and 26 old. Dashed line represents the Africa-Antarctica velocity vector between anomalies 26 old and 24 young, as predicted by *Royer et al.* [1988].

In and the SWIR fracture zone display a more acute angle with the SEIR and CIR spreading direction. This angle is about 30°, compared to 55° between anomalies 24 and 21. Such a configuration is more unstable and is likely to be associated with frequent TJ jumps, as required to maintain a pseudo-RRF mode.

The unstable pseudo-RRF mode results in frequent TJ jumps which create new SWIR compartments (Figure 11a). In order to account for the regional TJT-In direction, an unstable RRR model should also include frequent TJ jumps interrupting the fast eastward SWIR lengthening by the initiation of new SWIR fracture zones (Figure 11b). Both the unstable RRR and pseudo-RRF mode lead to similar TJ geometries. In the first, the current TJ configuration is RRR with a transient RRF configuration at the TJ jumps, while in the second, the current TJ configuration is pseudo-RRF with a transient RRR configuration at the TJ jumps. Data are too sparse to allow for clear discrimination between these models; a detailed survey of the TJ traces is required. As the spacing of the magnetic lineations is probably too large

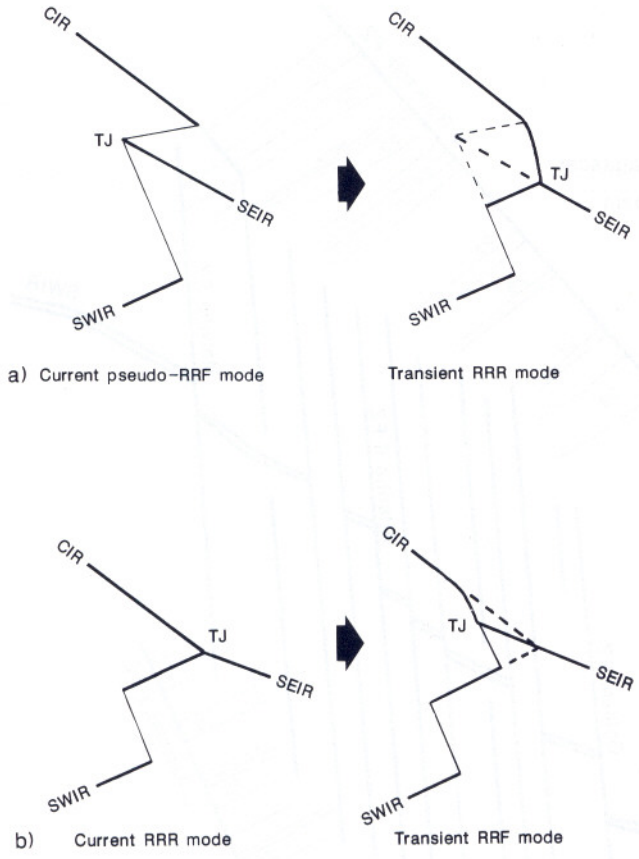

Fig. 11. Transient ridge-ridge-ridge to current pseudo-ridge-ridge-fault configurations, or transient ridge-ridge-fault to current ridge-ridge-ridge configurations between anomalies 28 old and 24 young?

to accurately resolve the TJ traces, basement topography, covered by sediments, needs to be investigated by seismic profiling.

Both the unstable RRR and the pseudo-RRF modes imply frequent ridge jumps and creation of new SWIR fracture zones and compartments. These models agree closely with SWIR physiography, which is characterized by numerous fracture zones between 52°30'E and 61°E, in an area created between anomalies 29 and 20 (Figure 12). These fracture zones, spaced at 70 km, are not solely related to the strong obliquity of the SWIR spreading direction with respect to the general orientation of the ridge. Farther west, the same obliquity is accommodated by some broad fracture zones, spaced at 500 km. We propose that numerous SWIR fracture zones between 52°30'E and 61°E are consequences of SWIR lengthening and therefore of the TJ evolution.

Oceanic crust created by SWIR lengthening between anomalies 29 and 24 presently lies between 52°30'E and 59°30'E. This area shows about 10 fracture zones quite regularly spaced, the mean spacing being 70 km. If these fracture zones were created by TJ jumps, their frequency is about one TJ jump per million year, as about 10 m.y. separates anomalies 29 and 24 in the geomagnetic reversal time scale. During the same time span, more than 700 km of oceanic crust were created by the CIR and the SEIR in the Central Indian Basin. Assuming a N353°E regional TJT-In direction and, as predicted by the RFF mode, a N60°E local TJT-In, geometrical considerations show that a total east-west readjustment of 1300 km is required to reconcile these directions. Such a readjustment corresponds to ten 130 km eastward TJ jumps, associated with 10 new SWIR fracture zones in the pseudo-RRF mode. Computed spacing of these fracture zones is about 70 km, in agreement with that observed. Considering the N20°W local TJT-In direction predicted by the RRR mode leads to a total east-west readjustment of 175 km, or ten 17.5 km eastward TJ jumps. As the SWIR lengthens at 40 km/m.y., the SWIR fracture zone spacing is therefore 40 km, a rather small value with respect to the measured one.

The previous calculations agree with the formation of closely spaced SWIR fracture zones at the TJ between anomalies 29 and 24. This conclusion suggests that the SWIR physiography reflects the past TJ configurations and therefore records the TJ history.

Concluding Discussion

The Central Indian Ocean Triple Junction (TJ) history may be summarized as follows. At anomaly 29, the TJ rapidly migrated eastward and located between La Boussole FZ and L'Astrolabe FZ; before, between anomalies 33 and 30, it lay in the eastern Mascarene Basin, about 300 km west of La Boussole FZ [*Dyment*, 1991]. Between anomalies 29 and 24, the TJ followed either an unstable ridge-ridge-ridge or, more likely, a pseudo-ridge-ridge-fault mode (Figure 11). A TJ jump every 1 m.y. resulted in the creation of ten 70 km spaced SWIR fracture zones, including Gallieni FZ and Atlantis II FZ (Figure 12). After a TJ jump at anomaly 24 young, a ridge-fault-fault mode prevailed (Figure 7), as shown by the N38°E CIR-SEIR offset in the Central Indian Basin (Figure 2) and its N-S conjugate in the Madagascar Basin (Figure 5). The CIR-SEIR offset reached a propagatorlike configuration, and the TJ remained stable for 3 m.y., until anomaly 22 young (Figure 8). The TJ jumped again before anomaly 21 old and created the last major SWIR fracture zone, Melville FZ, which presently lies at about 61°E (Figure 12). The Indian Ocean spreading system, and thus the TJ configuration, were strongly modified between anomalies 20 and 18. The part of the SWIR created after this major reorganization (i.e., east of 61°E) is not affected by large offset fracture zones.

Propagating rifts are likely to play an important role in triple junction evolution, as shown for the TJ between anomalies 24 and 21 and probably between anomalies 28 to 24. They offer numerous possibilities to solve velocity triangles using nonstationary offsets and allow another class of stable triple junction configurations. When several different configurations agree with the same velocity triangle, the existing configuration is likely to be the one which involves either the maximum tensile stress direction at the ridge axes or the minimal total power dissipation (see *Kleinrock and Phipps Morgan* [1988] for a discussion of these criteria).

New segments of spreading center are created either by breakup of continental (or older oceanic) lithosphere or by lengthening of an existing spreading center at ridge-ridge-ridge (at regional scale) triple junctions. About 5-10% of the total length of present spreading centers were created by the latter, including parts of the ridges abuting the Bouvet, Rodriguez, and Galapagos triple junctions. A large part of the Pacific Ocean may have been created by ridge lengthening at three RRR triple junctions [*Hilde et al.*, 1977]. Regional geometry of many spreading centers is unherited from breakup [e.g., *Munschy et al.*, 1992]; in a similar way, the association

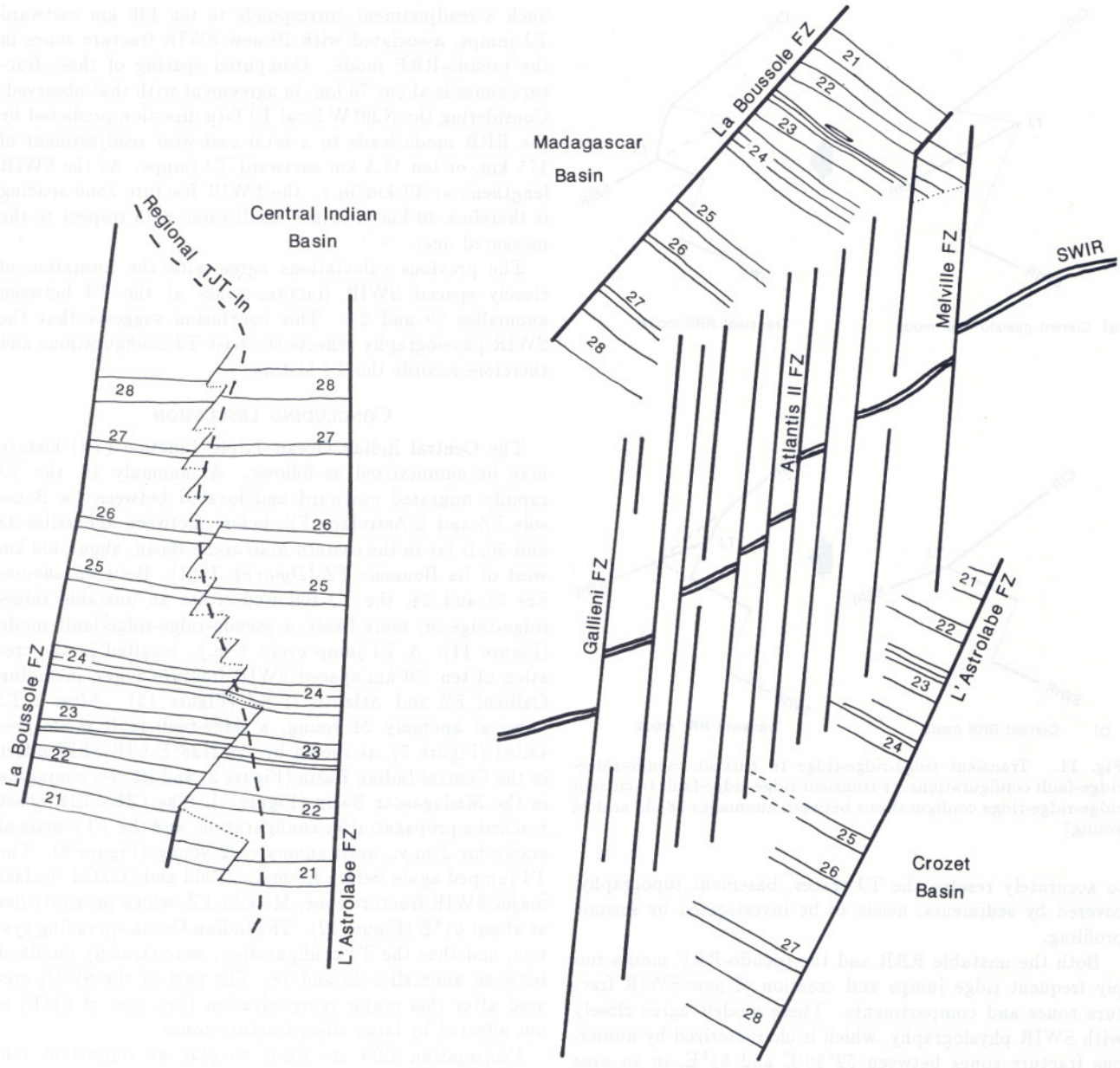

Fig. 12. Predicted configuration of (left) the Central Indian Basin, (right) the Crozet Basin, the Madagascar Basin and the Southwest Indian Ridge assuming that the ridge-fault-fault (pseudo-ridge-ridge-fault) Triple Junction configuration prevailed between anomalies 28 old and 24 young.

of numerous SWIR fracture zones and TJ jumps between anomalies 29 and 24 suggests that the regional geometry of spreading centers created by ridge lengthening is ~~not~~ inherited from the triple junction configuration. Such a genetic relationship also exists between fracture zones observed on the American-Antarctic and Southwest Indian ridges and the Bouvet Triple Junction evolution [*Kleinrock and Phipps Morgan*, 1988], and may help to understand the detailed evolution of other triple junctions.

Acknowledgments. This research was made possible by grants from the French Ministry of Education (AER contract) and from Société de Secours des Amis des Sciences. The French and American data were available through the Indian Ocean Data Compilation program (Principal Investigators: R. Schlich, J.G. Sclater, R.L. Fisher, S.C Cande, M.F. Coffin, and H. Bergh). I thank P. Patriat and M. Munschy for their review of an early draft of this paper, as well as two JGR anonymous reviewers and JGR associate editor M.F. Coffin for helpful comments and numerous corrections of the initial "frenglish" text. Special thanks are also due to M. Blanck for drafting most of the figures and to B. Fritsch for his help.

REFERENCES

Berggren, W.A., D.V. Kent, J.J. Flynn, and J.A. Van Couvering, Cenozoic geochronology, *Geol. Soc. Am. Bull., 96,* 1407-1418, 1985.

De Ribet, B., and P. Patriat, La région axiale de la dorsale sud-ouest indienne entre 53°Est et 59°Est: son évolution depuis 10 Ma, *Mar. Geophys. Res., 10,* 139-156, 1988.

Dyment, J., Structure et évolution de la lithosphère océanique dans l'océan Indien: Apport des anomalies magnétiques, thèse doct., 374 pp., Univ. L. Pasteur, Strasbourg, 1991.

Fisher, R.L., J.G. Sclater, and D.P. McKenzie, Evolution of the Central Indian Ridge, western Indian Ocean, *Geol. Soc. Am. Bull., 82,* 553-562, 1971.

Fisher, R.L., and J.G. Sclater, Tectonic evolution of the Southwest Indian Ocean since the Mid-Cretaceous: Plate motions and stability of the pole of Antarctica/Africa for at least 80 Myr, *Geophys. J. R. Astron. Soc., 73,* 553-576, 1983.

Fisher, R.L., M.Z. Jantsch, and R.L. Comer, General bathymetric chart of the oceans (GEBCO), sheet 5.09, Can. Hydrogr. Serv., Ottawa, 1982.

Hey, R.N., A new class of "pseudofaults" and their bearing on plate tectonics: A propagating rift model, *Earth Planet. Sci. Lett., 37,* 321-325, 1977.

Hey, R.N., G.L. Johnson, and A. Lowrie, Recent plate motions in the Galapagos area, *Geol. Soc. Am. Bull., 88,* 1385-1403, 1977.

Hey, R.N., F.K. Duennebier, and W.J. Morgan, Propagating rifts on midocean ridges, *J. Geophys. Res., 85,* 3647-3658, 1980.

Hey, R.N., M.C. Kleinrock, S.P. Miller, T.M. Atwater, and R.C. Searle, SeaBeam/Deep-Tow investigation of an active oceanic propagating rift system, Galapagos 95.5°W, *J. Geophys. Res., 91,* 3369-3393, 1986.

Hey, R.N., H.W. Menard, T.M. Atwater, and D.W. Caress, Changes in direction of seafloor spreading revisited, *J. Geophys. Res., 93,* 2803-2811, 1988.

Hilde, T.W.C., S. Uyeda, and L. Kroenke, Evolution of the Western Pacific and its margin, *Tectonophysics, 38,* 145-165, 1977.

Kamesh Raju, K.A., and T. Ramprasad, Magnetic lineations in the Central Indian Basin for the period A24-A21: A study in relation to the Indian Ocean Triple Junction trace, *Earth Planet. Sci. Lett., 95,* 395-402, 1989.

Kleinrock, M.C., and J. Phipps Morgan, Triple junction reorganization, *J. Geophys. Res., 93,* 2981-2996, 1988.

Macdonald, K.C., P.J. Fox, L.J. Perram, M.F. Eisen, R.M. Haymon, S.P. Miller, S.M. Carbotte, M.H. Cormier, and A.N. Shor, A new view of the mid-ocean ridge from the behaviour of ridge-axis discontinuities, *Nature, 335,* 217-225, 1988.

McKenzie, D.P., The geometry of propagating rifts, *Earth Planet. Sci. Lett., 77,* 176-186, 1986.

McKenzie, D.P., and W.J. Morgan, Evolution of triple junctions, *Nature, 224,* 125-133, 1969.

McKenzie, D.P., and J.G. Sclater, The evolution of the Indian Ocean since the Late Cretaceous, *Geophys. J. R. Astron. Soc., 25,* 437-528, 1971.

Mitchell, N.C., Distributed extension at the Indian Ocean Triple Junction, *J. Geophys. Res., 96,* 8019-8043, 1991.

Munschy, M., and R. Schlich, The Rodriguez Triple Junction (Indian Ocean): Structure and evolution for the past one million years, *Mar. Geophys. Res., 11,* 1-14, 1989.

Munschy, M., J. Dyment, M.O. Boulanger, D. Boulanger, J.D. Tissot, R. Schlich, Y. Rotstein, and M.F. Coffin, Breakup and seafloor spreading between the Kerguelen Plateau and Broken Ridge-Diamantina Zone, *Proc. Ocean Drill. Program, Sci. Results, 120,* 931-944, 1992.

Patriat, P., *Reconstitution de l'Evolution du Système de Dorsales de l'Océan Indien par les Méthodes de la Cinématique des Plaques,* 308 pp., Territoire des Terres Australes et Antarctiques Françaises, Paris, 1987.

Patriat, P., and V. Courtillot, On the stability of triple junctions and its relation to episodicity in spreading, *Tectonics, 3,* 317-332, 1984.

Patriat, P., and L. Parson, A survey of the Indian Ocean Triple Junction trace within the Antarctic plate: Implications for the junction evolution since 15 Ma, *Mar. Geophys. Res., 11,* 89-100, 1989.

Patriat, P., and J. Segoufin, Reconstruction of the Central Indian Ocean, *Tectonophysics, 155,* 211-234, 1988.

Royer, J.-Y., and R. Schlich, Southeast Indian Ridge between the Rodriguez Triple Junction and the Amsterdam and Saint Paul Islands: Detailed kinematics for the past 20 m.y., *J. Geophys. Res., 93,* 13524-13550, 1988.

Royer, J.-Y., P. Patriat, H.W. Bergh, and C.R. Scotese, Evolution of the Southwest Indian Ridge from the Late Cretaceous (anomaly 34) to the middle Eocene (anomaly 20), *Tectonophysics, 155,* 235-260, 1988.

Schlich, R., Structure et âge de l'océan Indien occidental, *Mem. Soc. Géol. Fr., 6,* 103 pp., 1975.

Schlich, R., The Indian Ocean: aseismic ridges, spreading centers, and oceanic basins, in vol. VI, *Ocean Basins and Margins, The Indian Ocean,* edited by A.E.M. Nairn, and F.G. Stehli, pp. 51-147, Plenum, New York, 1982.

Schlich, R., et al., Résultats préliminaires de la campagne océanographique Marion-Dufresne 61 sur la dorsale centrale-indienne entre 21° et 25°30'S, *C. R. Acad. Sci., 309,* 1765-1772, 1989.

Sclater, J.G., and R.L. Fisher, Evolution of the East Central Indian Ocean, with emphasis on the tectonic setting of the Ninetyeast Ridge, *Geol. Soc. Am. Bull., 85,* 683-702, 1974.

Sclater, J.G., B.P. Luyendyk, and L. Meinke, Magnetic lineations in the southern part of the Central Indian Basin, *Geol. Soc. Am. Bull., 87,* 371-378, 1976.

Sclater, J.G., R.L. Fisher, P. Patriat, C.R. Tapscott, and B. Parsons, Eocene to recent development of the South-west Indian Ridge, a consequence of the evolution of the Indian Ocean Triple Junction, *Geophys. J. R. Astron. Soc., 64,* 587-604, 1981.

Searle, R.C., and R.N. Hey, Gloria observations of the propagating rift at 95.5W on the Cocos-Nazca spreading center, *J. Geophys. Res., 88,* 6433-6447, 1983.

Tapscott, C.R., P. Patriat, R.L. Fisher, J.G. Sclater, H. Hoskins, and B. Parsons, The Indian Ocean Triple Junction, *J. Geophys. Res., 85,* 4723-4739, 1980.

Wilson, D.S., Tectonic history of the Juan de Fuca Ridge over the last 40 million years, *J. Geophys. Res., 93,* 11,863-11,876, 1988.

Wilson, D.S., R.N. Hey, and C. Nishimura, Propagation as a mechanism of reorientation of the Juan de Fuca Ridge, *J. Geophys. Res., 89,* 9215-9225, 1984.

J. Dyment, Earth and Planetary Sciences, McGill University, 3450 University, Montréal, PQ H3A-2A7, Canada

(Received April 23, 1992;
revised February 5, 1993;
accepted February 18, 1993.)